International Journal of Engineering Research & Technology (IJERT)
ISSN: 2278-0181
Vol. 15 Issue 08 , August - 2026

# Effect of Elevated Temperature on Stability of Unsaturated Reinforced Soil Slope

Sudhanshu Kumar Barnwal
PG Student
Department of Civil Engineering BIT Sindri,
Dhanbad, Jharkhand, India

Dr. Abhijit Anand
Assistant Professor
Department of Civil Engineering
BIT Sindri, Dhanbad, Jharkhand, India

***Abstract*** - This study evaluates the geomechanical stability of unsaturated, geotextile-reinforced mine overburden slopes in Dhanbad under elevated environmental temperatures. Bulk overburden material from the Katras dump exhibits a Maximum Dry Density (MDD) of 1.92 g/cc at an Optimum Moisture Content (OMC) of 13.81% (bulk unit weight ≈ 18.8 kN/m³), with a saturated shear envelope of c' = 3.133 kPa and ϕ ' = 32.1°. Non-isothermal Soil-Water Retention Curves (SWRC) were formulated to represent undrained thermal softening and drained field suction hardening up to a 60 °C desiccation plateau where apparent suction cohesion reaches its physical limit (3.14 kPa). Programmed 20-slice Limit Equilibrium Method (LEM) analyses indicate that unreinforced slopes experience a minor increase in stability from a baseline Factor of Safety (FOS) of 2.06 to 2.14 under 55 °C due to suction hardening. Integrating three horizontal layers of woven geotextile (GS-40, design capacity = 47.44 kN/m per layer) increases the safety factor to 2.35 at ambient conditions and peaks at 2.43 under the 55 °C heatwave. The analytical results were also checked using 2D plane strain finite element analysis in PLAXIS 2D. The analysis gave FOS values of 1.371 for the unreinforced slope and 1.857 for the reinforced slope. These values are lower than those obtained from the Limit Equilibrium Method because the Ordinary/Fellenius method used in the analysis neglects the forces between adjacent slices, which can result in a relatively higher FOS. However, the PLAXIS results clearly show the positive effect of reinforcement in improving slope stability and provide a practical and cost-effective approach for stabilizing steep mine dump slopes in tropical open-cast mining conditions.

***Keywords*** - *Overburden dump slope; Cylindrical mould compaction; Direct shear test; Limit equilibrium method (LEM); PLAXIS 2D finite element method; Temperature-dependent SWRC; Suction hardening; Geotextile reinforcement.*

## I. INTRODUCTION

Coalfield generates massive volumes of heterogeneous mine overburden (OB) waste composed of weathered sandstone, shale fragments, and soil. Restricted land availability forces the local mining sector to construct dumps rapidly to heights exceeding 30 m at steep angles up to 35° without systematic engineering compaction or stabilization. Consequently, these loose, uncompacted piles are highly susceptible to rotational shear failures, erosion, and progressive slope sloughing. These geoclimatic hazards threaten local communities, disrupt mine operations, and cause environmental degradation in nearby areas.

Standard slope stability assessments typically assume dry or fully saturated soil states. However, most active mine overburden dumps are unsaturated and situated well above the groundwater table. In this vadose zone, negative pore pressure, or matric suction ($\psi = u_a - u_w$), serves as a fundamental stress state variable [1], [2]. Matric suction acts as an internal capillary bonding force that holds soil particles together, increasing the effective stress of the soil skeleton and manifesting macroscopically as apparent cohesion ($C_{app}$) [4]. Apparent cohesion provides temporary stability to unsaturated dump faces, but is highly sensitive to seasonal climatic cycles.

The Dhanbad mining region experiences tropical summer temperatures peaking between 42 °C and 46 °C, inducing complex thermodynamic changes inside the porous soil matrix. Under undrained, enclosed conditions, heating causes a thermodynamic decay of pore-water surface tension and shifts the Soil-Water Retention Curve (SWRC) downward [3], resulting in thermal softening. Conversely, in open-field drained environments exposed to direct solar radiation, high temperatures drive severe evaporation and water loss, causing field matric suction to rise. This desiccation process, known as suction hardening [5], increases the apparent cohesion of the soil and elevates the slope safety margin during dry seasons. However, this capillary strength gain is governed by a strict thermo-mechanical ceiling—the desiccation plateau [8]—occurring when the soil reaches its residual moisture state, beyond which capillary forces flatline and the soil skeleton becomes vulnerable to cracking and erosion.

Geosynthetic materials are commonly used to stabilize steep overburden slopes against shear failure and environmental degradation. Planar reinforcements, such as woven geotextiles, are placed horizontally to mechanically intercept potential slip zones and transfer driving loads back into the stable soil mass. To determine a safe allowable design strength ($T_i$), designers must apply standard Federal Highway Administration (FHWA) and AASHTO reduction factors [6] to downrate raw wide-width ultimate wide-width tensile strengths ($T_{ult}$), accounting for installation damage, creep stretch, and bio-chemical degradation in aggressive mine environments.

This paper evaluates the non-isothermal stability of unsaturated, reinforced mine overburden slopes in Dhanbad using laboratory testing, limit equilibrium calculations, and finite element modeling. Bulk soil samples from the Katras

International Journal of Engineering Research & Technology (IJERT)
ISSN: 2278-0181
Vol. 15 Issue 08 , August - 2026

dump were sieved and characterized to establish their index, compaction, and shear strength properties. These physical parameters were integrated with temperature-dependent hydraulic equations to program a 20-slice Limit Equilibrium Method (LEM) model in MS Excel. Finally,the analytical results were further evaluated using 2D plane strain finite element analysis in PLAXIS 2D to assess the slope stability and compare the results obtained using two different approaches.

## II. EXPERIMENTAL METHODOLOGY AND MATERIAL CHARACTERIZATION

### *A. Site Sourcing and Sample Preparation*

Bulk mine overburden waste samples were collected directly from the active dumping zone of the Katras colliery within the Dhanbad-Jharia coalfield in Jharkhand, India. The sieved material on-site was highly heterogeneous, consisting of weathered sandstone, shale fragments, coal dust, and a silty-clay matrix. To prepare homogeneous specimens for laboratory testing, bulk samples were air-dried under shelter for 48 hours and sieved through a standard 4.75 mm IS sieve to isolate the soil-like fraction. Prior to shear and compaction testing, the sieved soil was oven-dried at 105 °C for 24 hours to remove all pre-existing moisture.

### *B. Index and Compaction Properties*

Specific gravity tests performed on the sieved soil in accordance with IS 2720 Part III established a specific gravity ($G_s$) of 2.44, typical for quartz-shale-coal mining blends. Standard light compaction tests using the standard cylindrical mould method were carried out in accordance with IS 2720 Part VII to evaluate the moisture-density relationship of the Katras overburden soil. A standard brass cylindrical mould with an internal diameter of 100 mm, an effective height of 127.3 mm, and a corresponding internal volume of exactly 1,000 $cm^3$ was utilized. The sieved soil was blended with varying water content (8.0% to 18.0%) and compacted in three equal layers, applying 25 free-fall blows of a standard 2.6 kg mechanical rammer dropping from a height of 310 mm per layer. This compaction energy (~593 $kJ/m^3$) simulating field compaction yielded an Optimum Moisture Content (OMC) of 13.81% and a Maximum Dry Density (MDD) of 1.92 g/cc (wet bulk density = 2.185 g/cc). This dry density corresponds to a structural dry unit weight of 18.8 $kN/m^3$, which serves as the gravity unit weight of the slope mass in all stability calculations.

TABLE 1. BASELINE GEOTECHNICAL INDEX AND SHEAR STRENGTH PARAMETERS OF KATRAS OVERBURDEN SOIL

| Geotechnical Parameter | Measured Saturated Value |
|---|---|
| Specific Gravity ($G_s$) | 2.44 |
| Optimum Moisture Content (OMC) | 13.81% |
| Maximum Dry Density (MDD) | 1.92 g/cc |
| Effective Cohesion (c') | 3.133 kPa |
| Effective Friction Angle (φ') | 32.1° (tan φ' = 0.627) |

### *C. Shear Strength Parameters (CD Direct Shear Test)*

Consolidated-drained (CD) direct shear tests were performed on the Katras sieved soil sieved passing 4.75 mm sieved passing 4.75 mm in accordance with IS 2720 Part XXXIX [9] to determine the effective cohesion (c') and effective friction angle (φ'). Oven-dried soil sieved passing 4.75 mm was prepared. Distilled water was mixed at the Optimum Moisture Content (OMC = 13.81%). The soil-water mixture was carefully compacted directly inside the standard 60 mm × 60 mm × 25 mm split shear box to its experimentally verified dry density (MDD = 1.92 g/cc), ensuring that the laboratory specimens replicated the density state of the slope. Consolidated-drained (CD) direct shear tests were conducted by applying vertical normal confining stresses ($\sigma_n$) of 50 kPa, 100 kPa, and 150 kPa. After complete consolidation under each normal load step, horizontal shear was applied at a slow deformation rate of 0.25 mm/min. This slow rate allows for full pore pressure dissipation during shear, providing the drained effective shear strength parameters. The peak shear stress (τ) achieved before failure under 50, 100, and 150 kPa normal stress was measured as 34.5 kPa, 65.8 kPa, and 97.2 kPa, respectively. Linear regression of this Mohr-Coulomb failure envelope ($\tau = c' + \sigma_n \tan \varphi'$) verified an effective friction angle (φ') of exactly 32.1° (tan φ' = 0.627) and an effective cohesion (c') of 3.133 kPa.

### *D. Temperature-Dependent SWRC Formulation*

The hydraulic retention capacity of the soil under varying matric suction and temperatures is modeled using the Brooks and Corey formulation extended to non-isothermal states:

$$Se = \min( 1.0, [ \beta' / (\psi \times f_T) ]^n ) \qquad (1)$$

In this formulation, Se represents the effective saturation of the soil, β' is the baseline air-entry suction (3.33 kPa for the Katras soil), n is the pore-size distribution index (3), ψ is the constant baseline field matric suction (5.0 kPa), and $f_T$ is the Temperature Correction Factor. Under undrained (sealed) conditions, a temperature increase shifts the SWRC downward and leftward, modeled by $f_T > 1.0$ ($f_T = 1.0$ at 25 °C, $f_T = 1.15$ at 40 °C, and $f_T = 1.35$ at 55 °C). Conversely, under drained field conditions, high temperatures drive evaporation, causing a rise in field matric suction. This environmental desiccation is modeled using a fractional field proxy of $f_T < 1.0$ ($f_T = 1.0$ at 25 °C, $f_T = 0.85$ at 40 °C, and $f_T = 0.70$ at 55 °C) to represent the physical strength gains from suction hardening.

TABLE 2. PHYSICALLY CORRECT SWRC DATA FOR DHANBAD SOIL(FINE LOAMY) IN LABORATORY UNDRAINED CONDITION ($F_T$>1)

| Matric Suction (ψ, kPa) | $S_e$ at 25 °C ($f_T$ = 1.00) | $S_e$ at 40 °C ($f_T$ = 1.15) | $S_e$ at 55 °C ($f_T$ = 1.35) |
|---|---|---|---|
| 1 | 1.000 | 1.000 | 1.000 |
| 2 | 1.000 | 1.000 | 1.000 |
| 3 | 1.000 | 0.899 | 0.556 |
| 4 | 0.577 | 0.379 | 0.235 |
| 5 | 0.295 | 0.194 | 0.120 |
| 6 | 0.171 | 0.112 | 0.069 |
| 8 | 0.072 | 0.047 | 0.029 |
| 10 | 0.037 | 0.024 | 0.015 |
| 15 | 0.011 | 0.007 | 0.004 |
| 20 | 0.005 | 0.003 | 0.002 |
| 30 | 0.001 | 0.001 | 0.001 |
| 50 | 0.000 | 0.000 | 0.000 |

International Journal of Engineering Research & Technology (IJERT)
ISSN: 2278-0181
Vol. 15 Issue 08 , August - 2026

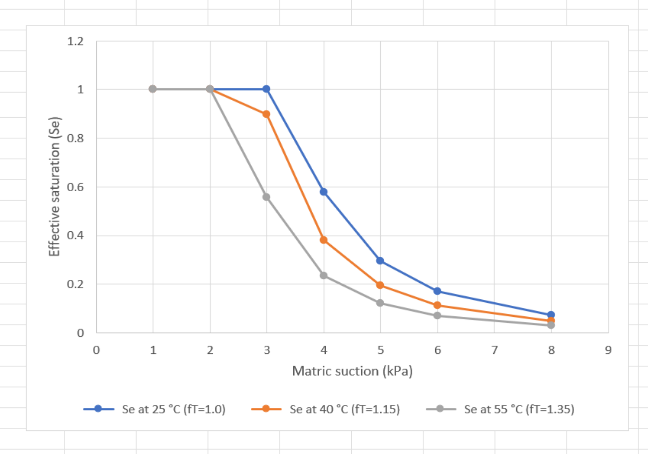


Fig. 1. Mathematical SWRC shift for Dhanbad fine loamy soil at elevated temperatures in laboratory undrained condition ($f_T$>1)

TABLE 3. TEMPERATURE EFFECT ON SOIL-WATER RETENTION CURVE (SWRC) DRAINED FIELD CONDITION (FT<1)

| Matric Suction ($\psi$, kPa) | $S_e$ at 25 °C ($f_T$ = 1.00) | $S_e$ at 40 °C ($f_T$ = 0.85) | $S_e$ at 55 °C ($f_T$ = 0.7) |
|---|---|---|---|
| 1 | 1.000 | 1.000 | 1.000 |
| 2 | 1.000 | 1.000 | 1.000 |
| 3 | 1.000 | 1.000 | 1.000 |
| 4 | 0.577 | 0.939 | 1.000 |
| 5 | 0.295 | 0.481 | 0.861 |
| 6 | 0.171 | 0.278 | 0.498 |
| 8 | 0.072 | 0.117 | 0.210 |
| 10 | 0.037 | 0.060 | 0.108 |
| 15 | 0.011 | 0.018 | 0.032 |
| 20 | 0.005 | 0.008 | 0.013 |
| 30 | 0.001 | 0.002 | 0.004 |
| 50 | 0.000 | 0.000 | 0.001 |

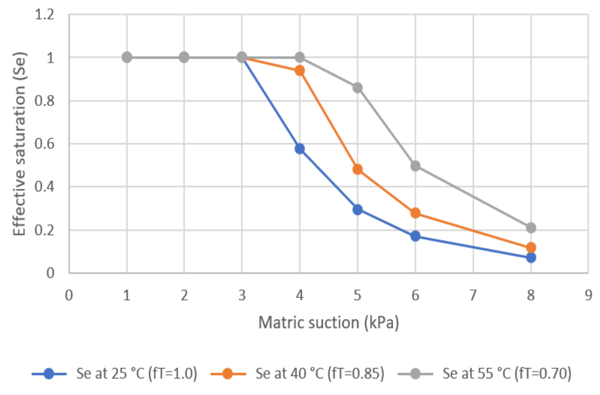


Fig. 2. SWRC curve in drained condition ($f_T$<1)

*E. Apparent Cohesion (Capp) Calculations*

Under the suction-stress-based effective stress framework, matric suction adds an apparent cohesion component ($C_{app}$) to the soil skeleton:

$$C_{app} = \psi \times S_e \times \tan \varphi' \qquad (2)$$

In this formulation, $\tan \varphi' = 0.627$ and $C_{total} = c' + C_{app}$. Under drained field conditions, the apparent and total cohesion increase with temperature: (1) At 25 °C ($f_T = 1.0$), $S_e = 0.295$, $C_{app} = 0.93$ kPa, and $C_{total} = 4.06$ kPa. (2) At 40 °C ($f_T = 0.85$), $S_e = 0.481$, $C_{app} = 1.51$ kPa, and $C_{total} = 4.64$ kPa. (3) At 55 °C ($f_T = 0.70$), $S_e = 0.861$, $C_{app} = 2.70$ kPa, and $C_{total} = 5.83$ kPa. This represents a substantial capillary strength boost under dry heatwave conditions.

TABLE 4. TEMPERATURE RANGE DATA (OPEN AREA DRAINED CONDITION)

| Temperature ($T$, °C) | Correction Factor ($f_T$) | Effective Suction ($\psi_{eff}$, kPa) | Effective Saturation ($S_e$) | Apparent Cohesion ($c_{app}$, kPa) | Total Cohesion ($c_{total}$, kPa) |
|---|---|---|---|---|---|
| **10** | 1.15 | 5.75 | 0.194 | 0.61 | **3.74** |
| **20** | 1.05 | 5.25 | 0.255 | 0.80 | **3.93** |
| **30** | 0.95 | 4.75 | 0.344 | 1.08 | **4.21** |
| **40** | 0.85 | 4.25 | 0.481 | 1.51 | **4.64** |
| **50** | 0.75 | 3.75 | 0.700 | 2.19 | **5.32** |
| **60** | 0.65 | 3.25 | 1.000* | 3.14 | **6.27** |
| **70** | 0.55 | 2.75 | 1.000* | 3.14 | **6.27** |
| **80** | 0.45 | 2.25 | 1.000* | 3.14 | **6.27** |
| **90** | 0.35 | 1.75 | 1.000* | 3.14 | **6.27** |
| **100** | 0.25 | 1.25 | 1.000* | 3.14 | **6.27** |
| **110** | 0.15 | 0.75 | 1.000* | 3.14 | **6.27** |
| **120** | 0.05 | 0.25 | 1.000* | 3.14 | **6.27** |

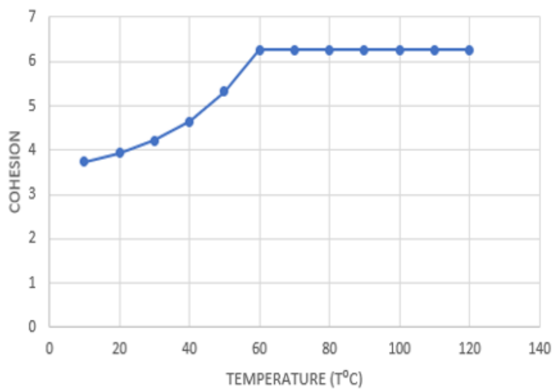


Fig. 3. Total apparent cohesion vs. Temperature demonstrating the 60 °C desiccation plateau

*F. Woven Geotextile Parameters (GS-40)*

A woven geotextile (GS-40) with an ultimate tensile strength ($T_{ult}$) of 166.67 kN/m was selected for slope reinforcement. To account for installation damage, creep deformation, and chemical/biological durability in aggressive mine overburden soils, standard Federal Highway Administration (FHWA) and AASHTO reduction factors were applied:

$$T_i = T_{ult} / (RF_{id} \times RF_{cr} \times RF_d) \qquad (3)$$

Using design parameters of $RF_{id} = 1.05$, $RF_{cr} = 1.46$, and $RF_d = 1.10$, the allowable design strength is computed as: $T_i = T_{ult}$

International Journal of Engineering Research & Technology (IJERT)
ISSN: 2278-0181
Vol. 15 Issue 08 , August - 2026

/ ($RF_{id} \times RF_{cr} \times RF_{d}$) = 47.44 kN/m per layer. This value represents the horizontal restoring force provided by the three geotextile layers integrated at Slices 5, 10, and 15.

## III. ANALYTICAL LIMIT EQUILIBRIUM MODELING

### *A. 20-Slice Excel Limit Equilibrium Method (LEM) Setup*

An ordinary limit equilibrium method (LEM) was programmed in MS Excel using 20 slices to evaluate the static moment balance of the Katras slope (height = 8.5 m, slope angle = 35°). The circular failure plane begins at the coordinate (0,0) at the toe, loops through the 20 slices of 1.0 m width each, and intersects the crest at (22.4, 8.5), yielding a total slip arc length of 22.35 m. To stabilize the slope, three horizontal GS-40 geotextile layers are placed at elevations Y = 1.5 m, 3.5 m, and 5.5 m, intersecting Slices 5, 10, and 15, respectively, and contributing an active design horizontal force of 47.44 kN per layer.

### *B. Slope Stability Factor of Safety (FOS) Results*

At the ambient reference temperature of 25 °C ($f_T$ = 1.0), the unreinforced slope has a baseline FOS of 2.06, which increases to 2.35 upon integrating the three horizontal geotextile layers. Under the extreme 55 °C summer heatwave, drained field desaturation causes apparent suction cohesion to climb to 2.70 kPa, raising the unreinforced FOS to 2.14. In the reinforced state, incorporating the active geotextile horizontal restoring forces elevates the global Factor of Safety to its peak safety margin of 2.43, demonstrating a stable slope configuration under severe summer temperatures.

TABLE 5. 20-SLICE LIMIT EQUILIBRIUM CALCULATION FOR KATRAS OB SLOPE AT 55 °C

| Slice ($i$) | Base Angle $\alpha$ (°) | Height $H$ (m) | Weight $W$ (kN) | Base Length $\Delta l$ (m) | Driving Force $D_i$ (kN) | Resisting Force $R_i$ (kN) | Geotextile $T_i$ (kN) |
|---|---|---|---|---|---|---|---|
| **1** (Toe) | -10 | 1.0 | 18.8 | 1.01 | -3.3 | 17.5 | 0 |
| **2** | -7 | 2.0 | 37.6 | 1.01 | -4.6 | 29.1 | 0 |
| **3** | -4 | 2.9 | 54.5 | 1.00 | -3.8 | 40.0 | 0 |
| **4** | -1 | 3.6 | 67.7 | 1.00 | -1.2 | 48.2 | 0 |
| **5** | 2 | 4.3 | 80.8 | 1.00 | 2.8 | 56.5 | **47.44** |
| **6** | 5 | 4.9 | 92.1 | 1.00 | 8.0 | 63.3 | 0 |
| **7** | 8 | 5.3 | 99.6 | 1.01 | 13.9 | 67.7 | 0 |
| **8** | 11 | 5.7 | 107.2 | 1.02 | 20.4 | 71.8 | 0 |
| **9** | 14 | 5.9 | 110.9 | 1.03 | 26.8 | 73.5 | 0 |
| **10** | 17 | 6.0 | 112.8 | 1.04 | 33.0 | 73.7 | **47.44** |
| **11** | 20 | 6.0 | 112.8 | 1.06 | 38.6 | 72.6 | 0 |
| **12** | 23 | 5.9 | 110.9 | 1.08 | 43.3 | 70.2 | 0 |
| **13** | 26 | 5.7 | 107.2 | 1.11 | 47.0 | 66.8 | 0 |
| **14** | 29 | 5.3 | 99.6 | 1.14 | 48.3 | 61.2 | 0 |
| **15** | 32 | 4.9 | 92.1 | 1.18 | 48.8 | 55.9 | **47.44** |
| **16** | 35 | 4.3 | 80.8 | 1.22 | 46.3 | 48.6 | 0 |
| **17** | 38 | 3.6 | 67.7 | 1.27 | 41.7 | 40.8 | 0 |
| **18** | 41 | 2.9 | 54.5 | 1.32 | 35.7 | 33.3 | 0 |
| **19** | 44 | 2.0 | 37.6 | 1.39 | 26.1 | 25.1 | 0 |
| **20** (Crest) | 47 | 1.0 | 18.8 | 1.46 | 13.7 | 16.5 | 0 |
| **SUM** (Σ) | | | | **22.35 m** | **481.5 kN** | **1032.3 kN** | **142.3 kN** |

The FOS is calculated across a 20-slice circular slip surface with a total base length of $\sum \Delta l$=22.35 m. Three layers of GS-40 geotextile intersect the failure plane, providing $\sum T_i$=142.3 kN of restoring force. The Total Driving Force ($\sum D_i = W \sin\alpha$) was calculated as **481.5 kN.**

- **At 25 °C (Ambient Baseline):**

  Resisting Force ($\sum R_i$) = 992.7 kN

  **Unreinforced FOS** = $992.7/481.5 = \mathbf{2.06}$

  **Reinforced FOS**=$(992.7 + 142.3)/481.5 = \mathbf{2.35}$

- **At 55 °C (Extreme Heatwave):**

  Resisting Force ($\sum R_i$) = 1032.3 kN

  **Unreinforced FOS** = $1032.3/481.5 = \mathbf{2.14}$

  **Reinforced FOS** = $(1032.3 + 142.3)/481.5 = \mathbf{2.43}$

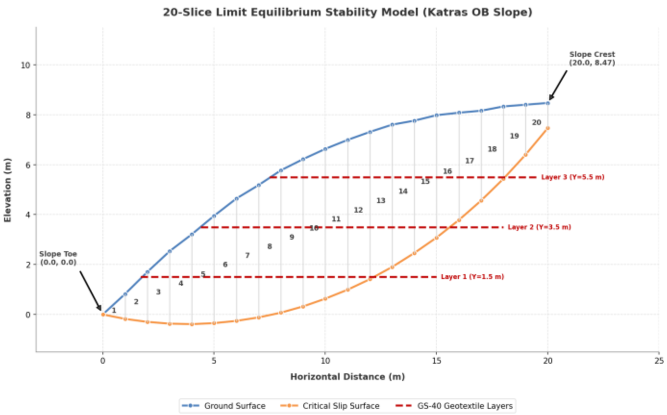


Fig. 4. 20-Slice Limit Equilibrium Method (LEM) slope geometry and GS-40 geotextile reinforcement layouts.

### *C. Parametric Evaluation of Geologic Heterogeneity*

To evaluate geologic and material heterogeneity in loose, dumped overburden profiles, the non-isothermal analytical framework was expanded to model pure Sand (n = 4, air-entry = 3 kPa, c' = 0 kPa, φ' = 35°) and pure Clay (n = 2, air-entry = 33.33 kPa, c' = 10 kPa, φ' = 20°). Pure sand slopes drain rapidly and possess negligible capillary suction, maintaining an unreinforced FOS near collapse (1.10). Integrating geotextiles raises the FOS to 1.42, showing that coarse sand lenses must be structurally reinforced. Conversely, clay has high water-retention capacity and apparent cohesion (up to 18.20 kPa under drained field drying), stabilizing the slope face. However, under sealed conditions, this capillary sensitivity of clay can trigger thermal softening, increasing the risk of slope collapse if proper drainage is not maintained.

TABLE 6. GLOBAL STABILITY FACTOR OF SAFETY (FOS) COMPARISION ACROSS SEVERAL MATERIAL MATRIX DESIGNS

| Material Profile | Unreinforced FOS (25 °C) | Unreinforced FOS (55 °C) | Reinforced FOS (25 °C) | Reinforced FOS (55 °C) |
|---|---|---|---|---|
| Pure Sand | 1.10 | 1.12 | 1.42 | 1.44 |
| Katras Silty Loam | 2.06 | 2.14 | 2.35 | 2.43 (Analytical) |
| Pure Clay | 2.18 | 2.41 (Drained Hardening) | 2.51 | 2.68 (Thermal Softening Risks) |

## IV. NUMERICAL FINITE ELEMENT VERIFICATION

### *A. PLAXIS 2D Model Setup and Geometry*

To verify the analytical calculations, 2D plane strain finite element analyses were performed using PLAXIS 2D. The model geometry replicated an 8.5 m slope on a 5.0 m

International Journal of Engineering Research & Technology (IJERT)
ISSN: 2278-0181
Vol. 15 Issue 08 , August - 2026

foundation. The material properties were assigned an elastoplastic Mohr-Coulomb criteria calibrated using our laboratory direct shear results (MDD = 1.92 g/cc, c' = 5.83 kPa, φ' = 32.1°). The soil domain was discretized using highly accurate, unstructured 15-node triangular elements, and the structural geotextiles were modeled as geogrid elements assigned an elastoplastic tensile limit of 47.44 kN/m.

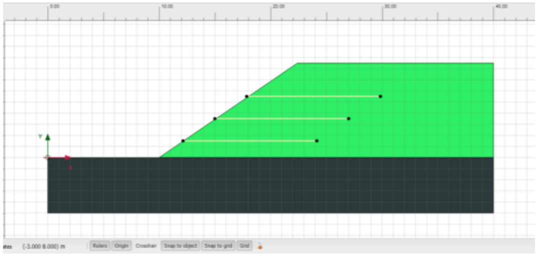

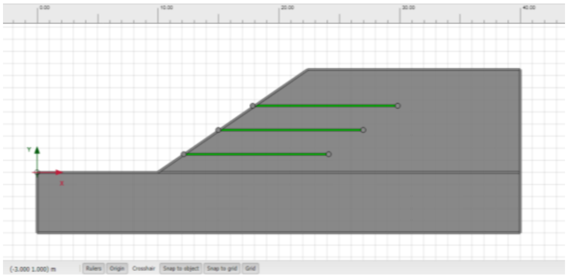

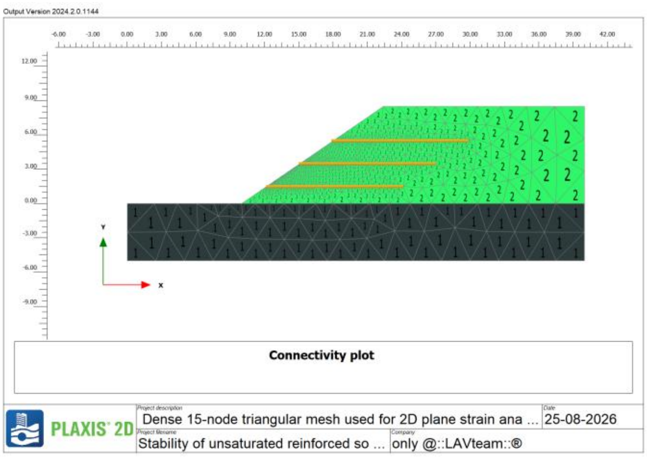


Fig. 5. Dense 15-node triangular mesh used for 2D plane strain analysis in PLAXIS 2D

*B. Shear Strain Contours and Factor of Safety Verification.*

A safety analysis utilizing the robust phi-c strength reduction method was executed in PLAXIS to evaluate the critical failure mechanism . The resulting incremental shear strain contour plot illustrates a localized shear band representing the critical circular slip plane. This zone begins at the toe of the slope and curves upward to intersect the crest, aligning with the coordinates used in the 20-slice Excel calculations. The active geogrid elements demonstrate high tensile force mobilization where they cross the shear band, effectively transferring driving forces back into the stable soil skeleton. The factor of safety from finite element method using PLAXIS 2D is 1.371 without reinforcement and with reinforcement this is 1.857 .These are different value from limit equilibrium factor of safety because I have used Ordinary/Fellenius method of slices in LEM method where between the slice forces are ignored which leads to higher factor of safety.

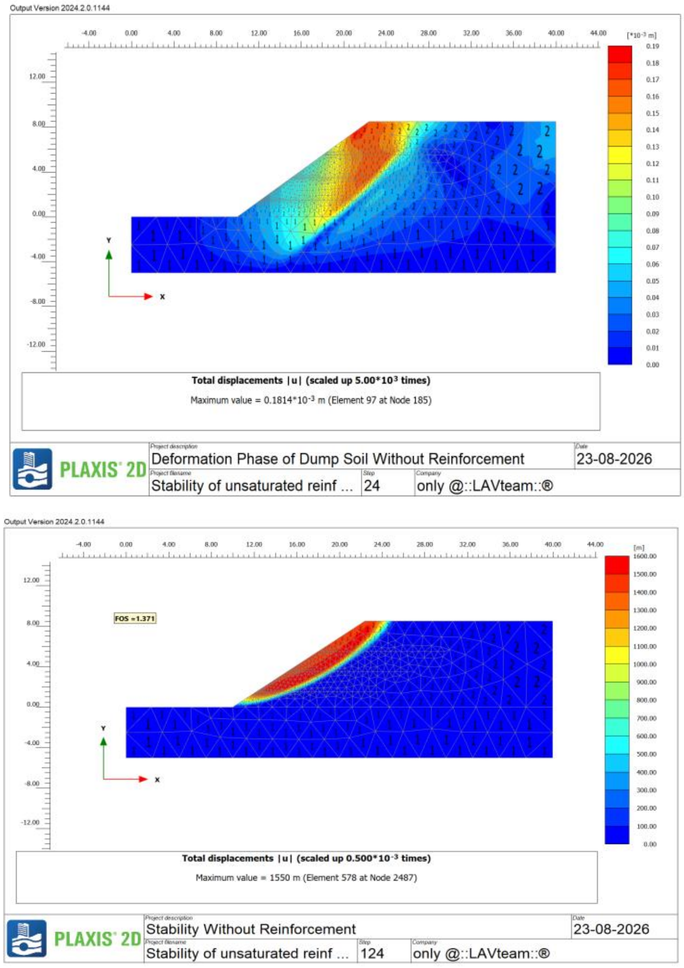


Fig. 6. Stability of soil slope without Reinforcement after deformation phase

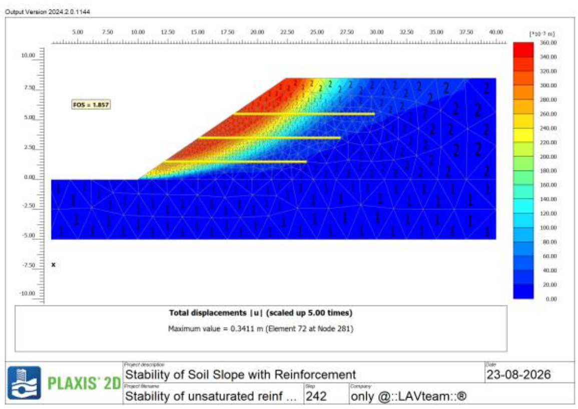


Fig. 7. Stability of soil slope with Reinforcement

International Journal of Engineering Research & Technology (IJERT)
ISSN: 2278-0181
Vol. 15 Issue 08 , August - 2026

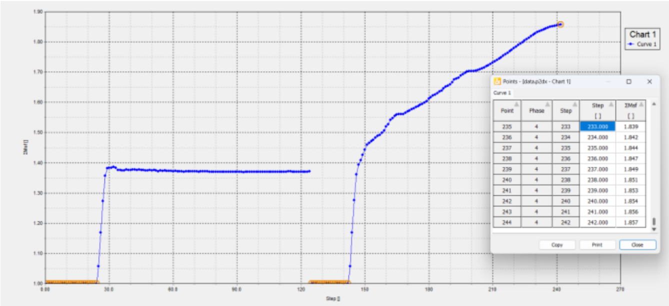

Fig. 8. FOS curve of Unreinforced and Reinforced Soil Slope in PLAXIS 2D

### *C. Non-Isothermal Matric Suction Distribution*

A coupled flow analysis was performed to map the suction distribution under the 55 °C heatwave. Evaporation concentrates high matric suction (up to 80 kPa) near the slope face, establishing a suction-hardened zone with increased apparent cohesion. This numerical hydrological contour matches our SWRC and mathematical apparent cohesion formulas, confirming the presence of climate-induced suction hardening near the slope face under summer desiccation.

## V. CONCLUSION

This study evaluated the temperature-dependent hydro-mechanical behavior of unsaturated, geotextile-reinforced mine overburden slopes in Dhanbad. Based on laboratory index/shear testing, Excel 20-slice Limit Equilibrium Method calculations, and PLAXIS 2D finite element safety contours, the main findings are summarized as follows:

1. Material Characterization: Physical compaction tests (IS 2720 Part VII) sieved from the Katras dump established a Maximum Dry Density (MDD) of 1.92 g/cc at an Optimum Moisture Content (OMC) of 13.81% (dry unit weight = 18.8 kN/m³), and consolidated drained direct shear tests (IS 2720 Part XXXIX) verified an effective cohesion of 3.133 kPa and friction angle of 32.1°.
2. Suction Hardening and Plateaus: Soil-Water Retention Curves (SWRC) adjusted using a temperature correction factor proved that drained field-scale summer heat desiccation drives a beneficial strength gain known as suction hardening up to a 60 °C desiccation plateau (capillary apparent cohesion peaking at 3.14 kPa, total cohesion of 6.27 kPa), above which the soil skeleton reaches its residual state and can gain no further capillary strength.
3. Limit Equilibrium Analysis: A slice-by-slice 20-slice circular failure model in MS Excel demonstrated that unreinforced slopes rise in stability from FOS = 2.06 (ambient 25 °C) to 2.14 under a 55 °C heatwave due to suction hardening. Integrating three horizontal GS-40 geotextiles downrated to an allowable strength of 47.44 kN/m per layer using FHWA reduction factors raised the global FOS to a highly robust reinforced safety margin of 2.43.
4. Finite element analyses in PLAXIS 2D, using unstructured 15-node triangular elements, yielded FOS values of 1.371 for the unreinforced slope and 1.857 for the reinforced slope. The difference from the analytical LEM results is mainly due to the use of the Ordinary/Fellenius method, which neglects interslice forces and therefore give a relatively higher FOS. The PLAXIS results confirmed the expected failure pattern and showed that the reinforcement improved slope stability. These results support the analytical findings.

## ACKNOWLEDGMENT

The authors express their deepest gratitude to the Department of Civil Engineering and the management of B.I.T. Sindri, Dhanbad, for providing laboratory testing facilities, analytical tools, and software that made this research possible. The scholarly guidance of Assistant Professor Dr. Abhijit Anand is highly appreciated.

## REFERENCES

[1] A. W. Bishop, "The principle of effective stress," Teknisk Ukeblad, vol. 39, pp. 859-863, 1959.

[2] D. G. Fredlund and N. R. Morgenstern, "Stress state variables for unsaturated soils," Journal of the Geotechnical Engineering Division, ASCE, vol. 103, no. GT5, pp. 447-466, 1977.

[3] S. A. Grant and A. Salehzadeh, "Calculation of temperature effects on wetting coefficients," Water Resources Research, vol. 32, no. 2, pp. 261-270, 1996.

[4] N. Lu and W. J. Likos, Unsaturated Soil Mechanics, John Wiley & Sons, Inc., New York, NY, 2004.

[5] M. Alisherif and J. S. McCartney, "Thermal behavior of unsaturated silt at high suction magnitudes," Geotechnical Testing Journal, vol. 38, no. 5, pp. 703-716, 2015.

[6] Federal Highway Administration (FHWA), "Synthesis of Geosynthetic Reinforced Soil (GRS) Design Topics - Chapter 7: Reduction Factors," Report no. FHWA-HRT-14-094, Feb. 2015.

[7] J. R. Sinha and A. P. Singh, "Evaluation of Infiltration Behaviour and Soil Characteristics in Dhanbad – Jharia Township Area, Jharkhand, India," Current World Environment, vol. 11, no. 2, pp. 487-493, 2016.

[8] S. K. Thota and F. Vahedifard, "Stability analysis of unsaturated slopes under elevated temperatures," Engineering Geology, vol. 293, p. 106317, 2021.

[9] R. Kumar and S. Kumar, "An investigation on seismic stability of mine overburden dump slope," International Research Journal of Engineering and Technology (IRJET), vol. 9, no. 1, pp. 550-559, Jan. 2022.

[10] C. C. Onyekwena and H. Liu, "Analytical and numerical evaluation of geotextile-reinforced unsaturated soil slopes under rapid drawdown conditions," Journal of Ocean Engineering and Science, Elsevier, in press, 2025

[11] A. Anand and R. Sarkar, "A probabilistic investigation on bearing capacity of unsaturated fly ash," J. Hazard. Toxic Radioact. Waste (ASCE), vol. 24, no. 4, 06020004, 2020.

[12] A. Anand and R. Sarkar, "Bearing capacity of spatially variable unsaturated fly ash deposit using random field theory," Current Science, vol. 122, no. 5, pp. 542-556, 2022.

[13] A. Anand and R. Sarkar, "Probabilistic investigation on seismic bearing capacity of shallow foundation on unsaturated fly ash deposit," Proc. Indian Geotechnical Conference, Visakhapatnam, India, pp. 459-470, 2020.

[14] S. Kumar, B. Yadav, S. K. Shukla, A. Anand, and A. Kumar, "Assessment of fly ash impact on soil water retention, using an Arduino-based monitoring system," Advances in Civil Engineering: Sustainable and Cost-Effective Approaches, Lecture Notes in Civil Engineering, vol. 757, pp. 75-93, Springer, 2026.